# HIGH-CYCLE FATIGUE AND CREEP OF THE CAST NICKELBASE SUPERALLOY IN738LC AT 850°C

H. Schmidt*, W. Hoffelner+

Interactions between high-cycle fatigue (HCF) and creep loading were investigated for the cast nickelbase-superalloy IN 738 LC. For this purpose HCF tests were performed at different mean stresses at 850°C. The results showed that we can decide between a stress-range dependent fatigue part and a mean stress dependent creep part. It was found that almost no coupling exists between these two parts so that the sample fails by fatigue at low mean stresses and by creep at high mean stresses. HCF can be understood as crack growth from defects; creep can be predicted by a Larson-Miller fit but it cannot be related to fracture mechanics quantities.

## INTRODUCTION

Centrifugal forces and vibrations are typical operating conditions of rotating machines such as gas turbines. They lead to creep deformation and high-cycle fatigue (HCF)-loading of the blades. A knowledge of creep and HCF properties of blading materials is therefore very important. For the cast nickelbase-superalloy IN 738 LC, a typical gas turbine blading material, the pure creep behaviour can be well represented by a Larson-Miller fit (1) or by a Spera approach (2) as shown by Buchmayr and Danzer (3). The pure fatigue region upto R-values of 0.3 (R = minimum stress $\sigma_{min}$ / maximum stress $\sigma_{max}$) can be understood in terms of crack growth from preexisting pores as recently demonstrated (4). However it was also shown there that this simple fracture mechanics model breaks down as soon as creep becomes important (R > 0.3). The present paper is aimed at understanding the interaction between HCF and creep.

## EXPERIMENTAL

The experiments were performed with the cast nickel-base superalloy IN 738 LC. This is a γ' hardened alloy containing mainly MC-carbides and $M_{23}C_6$-carbides as minor phases. The microstructure of this alloy has been studied extensively in the literature e.g. (5). Hour-glass specimens samples with a gauge diameter of 4.5 mm were machined out of cast blocks after conventional heat treatment (2 h/1120°C air cooling + 24 h/845°C air cooling). The fatigue tests were performed with an Amsler vibrophore fatigue machine at 850°C in air. The testing frequency was 170 Hz and the R-values varied between 0 and 0.9. After the tests the specimens were metallographically investigated.

* University of Vienna, Inst. Mat. Sci., Währingerstr. 42, A-1090 Vienna, Austria
+ BBC Brown, Boveri & Co., Research Center, CH-5405 Baden, Switzerland

## FATIGUE AND CREEP DATA

The results of the fatigue experiments are summarized in Figs. 1 and 2. Figure 1 shows the S/N curves at different R-ratios and Fig. 2 shows the $10^8$-endurance limits in a Smith-diagram. In this representation $\sigma_m \pm \sigma_a$ ($\sigma_m$, mean stress, $\sigma_a$, alternating stress amplitude) is plotted as a function of the mean stress, $\sigma_m$. The creep stress for a time equivalent to the considered number of cycles to failure is normally used as the limiting unidirectional load at high temperatures, where creep becomes important (160 hrs for a test frequency of 170 Hz).

Between R = -1 and R = 0 the upper part of the diagram remains fairly constant which means that the endurance limit in this R-range is mainly determined by the positive part of the stress. Between R = 0 and R = 0.3, the Smith-diagram is almost parallel to the 45-degrees line indicating that the endurance limits are only dependent on the applied stress range $\Delta\sigma$ and independent of the mean stress. As shown in a recent investigation (4), these parts of the diagram can be described by fatigue crack growth from preexisting casting pores. It was shown there that the $10^8$-endurance limits, $\Delta\sigma_o$, can be calculated from the simple fracture mechanics relation:

$$\Delta\sigma_o = \frac{\Delta K_o}{\sqrt{\pi \cdot a} \cdot Y} \qquad (1)$$

where $\Delta K_o$ is the fatigue threshold stress intensity range ($\Delta K_o \sim 3.8$ MN.m$^{-3/2}$ for this material), a is the average dimension of casting pores and Y is a geometry dependent function. Assuming that only the positive part of the stress range contributes to crack growth, we can explain the constant upper part of the Smith diagram between R = -1 and R = 0. Since the fatigue crack growth thresholds are almost independent of R between R = 0 and R = 0.3, the shape of the Smith diagram in this R-range can also be understood. However, with further increasing R-values this simple fracture mechanics model breaks down and creep of smooth samples cannot be described as creep crack growth from preexisting casting pores.

We therefore attempted to correlate the high R-values with stress rupture data of smooth samples. Considerable creep-data of smooth samples of this material has been produced as a result of intensive investigations of IN 738 LC in the framework of a European collaborative action COST-50. As already mentioned the creep rupture curves can be described well by the Spera method (2) or by the Larson-Miller equation (1). Since according to (3) almost no difference exists between these two fits for the 850°C data we will confine ourselves to the Larson-Miller fit:

$$t_f = t_{fo} \cdot \exp \frac{Q_c - V \cdot \sigma}{RT} \qquad (2)$$

In this equation $t_f$ is the stress rupture life, V the activation volume, $\sigma$ the stress, $Q_c$ the activation energy and $t_{fo}$ a constant. The values determined by Buchmayr and Danzer (3) were used as numerical values.

## SEPARATION OF CREEP AND FATIGUE

For the separation between creep and fatigue the mean stress $\sigma_m$ was assumed to be the creep stress $\sigma_c$, whereas the stress range $\Delta\sigma$ was assumed to describe the fatigue part. Although there is no direct physical basis for this very simple separation between creep and fatigue, it leads to a good description of

the results as will be shown. Figure 3 shows the S/N-curves in a representation where not the alternating stress $\sigma_a$, but the mean stress $\sigma_m$ is plotted as a function of the testing time, t. In this diagram the Larson-Miller creep curve was plotted for comparison. It can be seen from this plot that fatigue at R = 0.6 up to 0.9 can be simply understood as creep rupture under the applied mean load $\sigma_m$. For R = 0.3 we are far away from the creep curve at low number of cycles to failure $N_f$, but it can be easily seen that at high number of cycles the fatigue curve and the creep curve come together and it can be expected that for $N_f$ larger than $10^8$, the creep strength is the actual life determining quantity and consequently a drop of the fatigue curve with increasing numer of cycles can be expected. For R = 0 the mean stresses are obviously too low to cause a significant amount of creep up to $10^{10}$ cycles at this frequency. However, at about $2 \times 10^{10}$ cycles (which equals about $3.7 \times 10^4$ hours at this frequency) creep becomes important even at R = 0.

It is clear from these considerations that the Smith-diagram in the presented form is only of limited use in representing high-temperature fatigue data since it loses its significance at mean stresses where creep becomes important (≧ 850°C for IN 738 LC). This can also be seen from the large scatter of the values at R = 0.6 and R = 0.9 in Fig. 2. Confining ourselves to the $10^8$ endurance limit the Smith diagram should only be used up to R = 0.3 for IN 738 LC.

## FAILURE MECHANISMS

Metallographic investigations of the broken samples were performed to gain more insight into the mechanisms responsible for failure under different loading conditions. Typical results are shown in Figs. 4 a-c.

As expected (4, 6) the samples fail from preexisting casting pores under pure fatigue loading (Fig. 4a). In the early stage of propagation the fatigue crack propagates transgranularly showing a smooth fracture surface.

Figure 4c shows the fracture surface of a sample broken under high mean stress (R = 0.9). Here are no signs of a transgranularly and smoothly propagating fatigue crack. The fracture has mainly an interdendritic appearence as is typical for a creep crack in this material. This confirms the assumption that under these conditions the failure mechanism is pure creep.

A mixed situation is shown in Fig. 4b. Here a typical HCF-crack can be seen. However this crack did not start from a casting pore but from a surface defect which was obviously developed during creep. In other words, creep damage leading to nucleation of small surface cracks resulted from creep deformation under the applied mean load. As soon as one of these defects grew to a size leading to a cyclic stress intensity range, $\Delta K$, higher than the threshold stress intensity range $\Delta K_o$, this crack propagated further as a fatigue crack until final fracture occurred. It could be estimated from the fatigue crack growth results of this material shown e.g. in (4) that only a few percent of the total life of this sample was spent in fatigue crack propagation so that almost all of the lifetime was consumed by pure creep.

From these observations we can draw the conclusion that in this material the HCF-failure is always due to crack propagation from existing defects, either preexisting casting pores or surface cracks developed during creep under the applied mean load. However almost all the stress rupture life of the sample is consumed before the creep crack has grown to such an extent that it can propagate as a fatigue crack, so that the lifetime of the sample coincides with the lifetime expected from the stress rupture curve. At very high mean

stresses (R = 0.9) the maximum applied alternating loads would require about 2 mm crack length to exceed the fatigue threshold stress intensity range. This means fatigue crack growth could only occur during the last stage of fast final fracture so that in this case no signs of fatigue can be seen on the fracture surfaces and the stress rupture curve again determines completely the fatigue life.

## CONCLUDING REMARKS

It has been determined from HCF-experiments on the cast nickelbase-superalloy IN 738 LC at 850°C at different mean stresses that there are two distinct life-determining factors: The stress-range dependent fatigue part which can be understood as crack growth from defects and the mean-stress dependent creep part. In the pure fatigue situation fatigue life is governed completely by the size and location of casting pores, whereas the pure stress rupture behaviour can be described by a Larson-Miller fit and cannot be quantified in fracture mechanics terms. However, an almost complete separation of the two damage mechanisms was observed so that the specimen life is consumed either in fatigue or in creep but no significant interaction between these two loading conditions is expected for this material. It could also be shown that even down to an R-ratio of 0 no fatigue limit can be expected because the fatigue curve always crosses the creep curve. From this point of view a Smith-diagram is not a very useful representation of data as soon as creep becomes important.

## ACKNOWLEDGEMENT

This work was carried out during the visit of H. Schmidt at the Brown Boveri Research Center in Baden, Switzerland. The authors would like to thank Mr. H. Baldinger for technical assistance and Mrs. Z. Posedel for helpful assistance in performing the metallographic investigations. This work was performed within the framework of COST action 50 and was financed in part by the Swiss Federal Government.

## LITERATURE

1. Larson, F.R., Miller, J., 1952, Trans. Am. Soc. Mech. Eng., 74, 765.

2. Spera, D.A., 1969, NASA TN D-5317.

3. Buchmayr, B., Danzer, R., 1981 "Creep and Fatigue Behaviour of IN 738 LC", COST-50, Int. Rep. no. 1, Montanuniv. Leoben, A-8700 Leoben, Austria.

4. Hoffelner, W., 1982, Met. Trans., in press.

5. Hoffelner, W., Kny, E., Stickler, R., McCall, W.J., 1979, Z. Werkstofftechn., 10, 84.

6. Hoffelner, W., Tschegg, E., 1981, Z. Werkstofftechn., 12, 185.

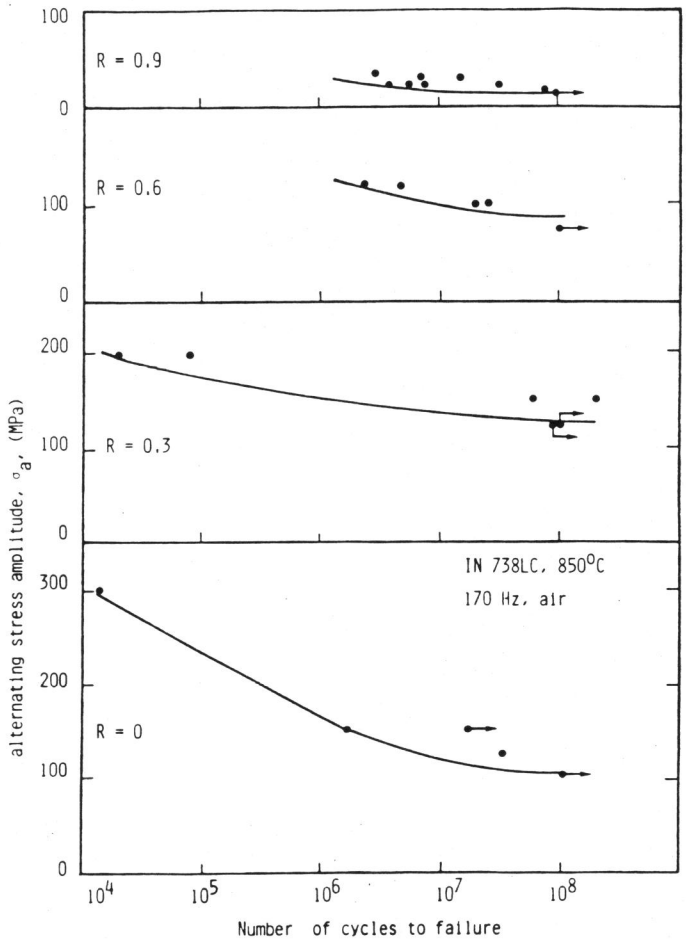


Figure 1 S/N-curves of IN 738 LC at different mean stresses.

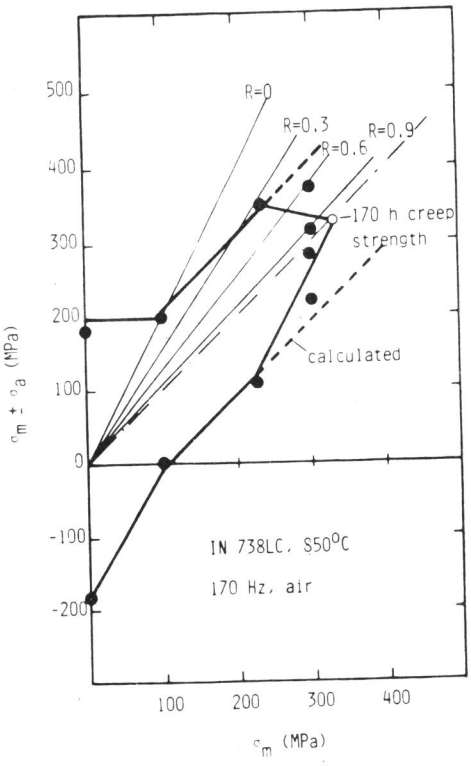


Figure 2 Smith diagram of IN 738 LC tested at 850°C. Calculated lines and value at R=-1 replotted from literature (4). The auxiliary lines (R=0, R=0.3, R=0.6, R=0.9) represent loci of constant R-values.

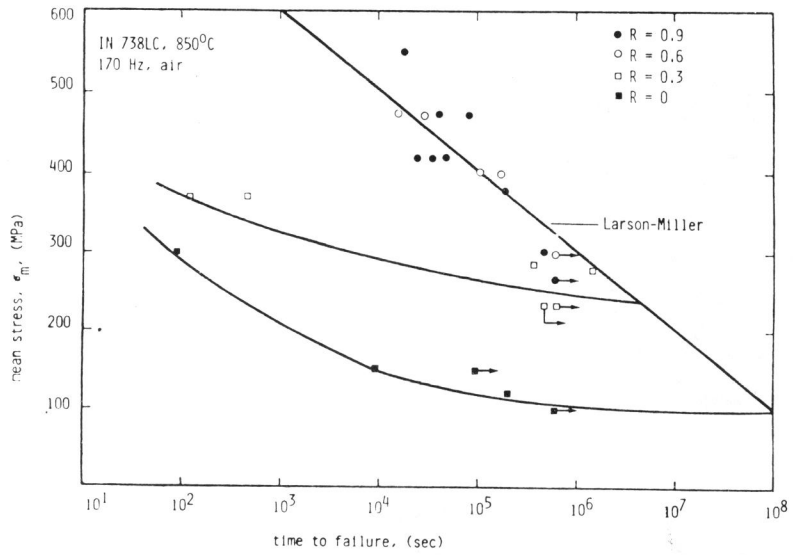


Figure 3 Time to failure (frequency × number of cycles) as a function of mean stress for IN 738 LC specimens tested in fatigue at 850°C at different R-values. Larson-Miller creep curve according to literature (3).

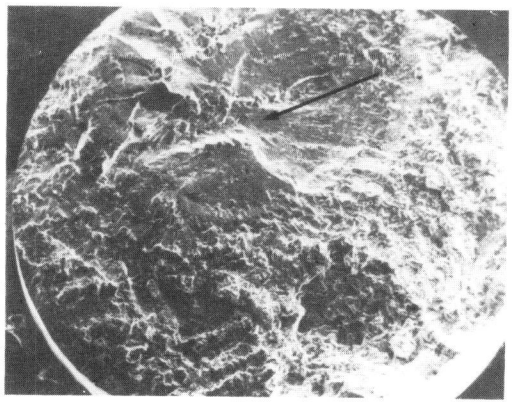

Figure 4a Fatigue crack starting from a casting pore (arrow). IN 738 LC, 850°C, 170 Hz, $\sigma_a$=150 MPa, R=0, N=1.6 · $10^6$.

1mm

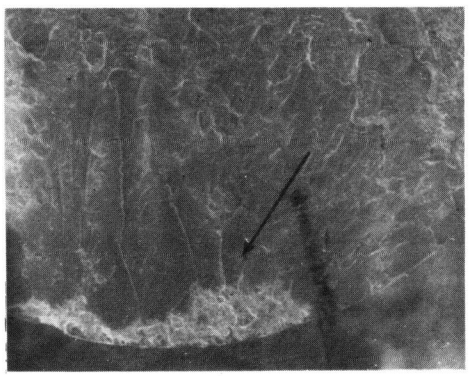

Figure 4b Fatigue crack starting from a creep induced defect (arrow). IN 738 LC, 850°C, 170 Hz, $\sigma_a$=119 MPa, R=0.6, N=4.9 · $10^6$.

0,5 mm

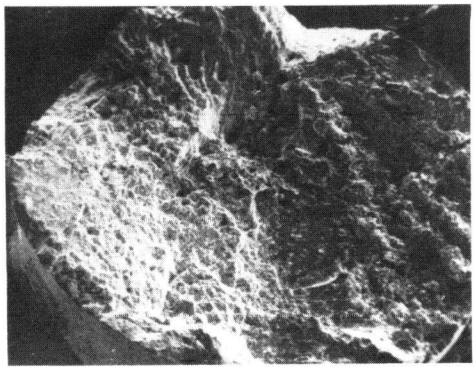

Figure 4c Fracture surface of IN 738 LC broken in fatigue at very high mean stress. 850°C, 170 Hz, $\sigma_a$=22 MPa, R=0.9, N=8 · $10^6$.

1mm